**OPEN**

# Molecular basis of fosmidomycin's action on the human malaria parasite *Plasmodium falciparum*

Tomonobu Umeda[1], Nobutada Tanaka[1], Yoshio Kusakabe[1], Masayuki Nakanishi[2], Yukio Kitade[3,4,5,6] & Kazuo T. Nakamura[1]

[1]School of Pharmacy, Showa University, Tokyo 142-8555, JAPAN, [2]College of Pharmaceutical Sciences, Matsuyama University, Ehime 790-8578, JAPAN, [3]Faculty of Engineering, [4]Center for Advanced Drug Research, [5]Center for Emerging Infectious Diseases, and [6]Graduate School of Drug Discovery and Medical Information Sciences, Gifu University, Gifu 501-1193, JAPAN.

The human malaria parasite *Plasmodium falciparum* is responsible for the deaths of more than a million people each year. Fosmidomycin has been proven to be efficient in the treatment of *P. falciparum* malaria by inhibiting 1-deoxy-D-xylulose 5-phosphate reductoisomerase (DXR), an enzyme of the non-mevalonate pathway, which is absent in humans. However, the structural details of DXR inhibition by fosmidomycin in *P. falciparum* are unknown. Here, we report the crystal structures of fosmidomycin-bound complete quaternary complexes of PfDXR. Our study revealed that (i) an intrinsic flexibility of the PfDXR molecule accounts for an induced-fit movement to accommodate the bound inhibitor in the active site and (ii) a *cis* arrangement of the oxygen atoms of the hydroxamate group of the bound inhibitor is essential for tight binding of the inhibitor to the active site metal. We expect the present structures to be useful guides for the design of more effective antimalarial compounds.

Malaria is one of the most widespread infectious diseases, with approximately 500 million cases and more than one million deaths per year[1]. Human malaria is caused by an infection with intracellular parasites of the genus *Plasmodium* that are transmitted by *Anopheles* mosquitoes[2]. *Plasmodium falciparum* is the most lethal of the four species of *Plasmodium* that infect humans. *P. falciparum* has become highly resistant to a wide variety of antimalarial drugs, such as chloroquine, amodiaquine, and sulphadoxine-pyrimethamine. New antimalarial drugs with novel modes of action are urgently needed for the treatment of multidrug-resistant *P. falciparum* malaria.

The isoprenoid precursors isopentenyl diphosphate and dimethylallyl diphosphate are synthesised by either the classical mevalonate pathway or the newly discovered nonmevalonate pathway (the 1-deoxy-D-xylulose 5-phosphate (DOXP) pathway, also called the 2-*C*-methyl-D-erythritol 4-phosphate (MEP) pathway). The DOXP pathway has been detected in eubacteria, higher plants, algae, cyanobacteria, and diatoms[3,4]. This pathway is also present in the apicoplast of *P. falciparum*[5]. The DOXP pathway is an ideal target for the development of herbicides and antibacterial drugs because it is essential for plants, eubacteria[6–8], and protozoa[9], but it is not found in animals.

The second enzyme of the DOXP pathway, DOXP reductoisomerase (DXR; EC 1.1.1.267), catalyses the NADPH- and divalent cation ($Mg^{2+}$ or $Mn^{2+}$)-dependent transformation of DOXP into MEP[10,11]. Shortly after the discovery of DXR, it was reported that the antibiotic fosmidomycin [3-(*N*-formyl-*N*-hydroxyamino)propyl-phosphonate], originally isolated from *Streptomyces lavendulae*, was a potent inhibitor of this enzyme (Fig. 1)[12]. In 1999, Jomaa and co-workers reported that fosmidomycin and FR900098 (an *N*-acetyl derivative of fosmido-mycin) were able to (1) inhibit the enzymatic activity of recombinant DXR from *P. falciparum* (PfDXR), (2) suppress the growth of *P. falciparum* in culture, and (3) cure mice infected with a related malaria parasite, *Plasmodium vinckei*[5]. These data established that PfDXR is a promising anti-malarial target. Clinical phase II trials using fosmidomycin alone or in combination with clindamycin conducted in Gabon and Thailand demonstrated that PfDXR is an effective target of the chemotherapy used to treat uncomplicated malaria[13–15]. However, malarial recrudescence is a common problem because it is difficult to completely eradicate malaria parasites from the human body. Therefore, the refinement of the anti-malarial performance of fosmidomycin alone or in combination with another compound is expected to lead to more effective anti-malarial drugs.

To date, several crystal structures of DXR from *E. coli*[16–20], *Z. mobilis*[21], *M. tuberculosis*[22], and *T. maritima*[23] have been reported. However, the crystal structures of the fosmidomycin-target enzyme PfDXR (when using fosmidomycin as an antimalarial drug) and the complete quaternary (enzyme-NADPH-metal-inhibitor) complex of DXR have not yet been reported. Here, we report the crystal structures of PfDXR in the absence and presence of antimalarial drugs. The complete quaternary complexes revealed that a *cis* arrangement of the oxygen atoms in the hydroxamate group of the bound inhibitor is essential for tight binding of the inhibitor. The results provide insight for the rational design of more effective PfDXR inhibitors.

## Results

**Overall structure.** In its active form (Lys75 to Ser488), the PfDXR enzyme is a homo dimer in which each subunit contains an NADPH molecule and a divalent metal ion. Its molecular mass is approximately 47 kDa. The crystal structures of PfDXR in an inhibitor-free ternary complex with NADPH and $Mn^{2+}$, a fosmidomycin-bound quaternary complex with NADPH and $Mg^{2+}$ (fosmidomycin, Fig. 1), and an FR900098-bound quaternary complex with NADPH and $Mg^{2+}$ (FR900098, *N*-acetyl derivative of fosmidomycin, Fig. 1) were determined at 1.86-, 1.9-, and 2.15-Å resolutions, respectively. The overall structure of PfDXR is essentially similar to those of DXRs from other species[16–23]. For simplicity, the following description refers primarily to subunit A of the fosmidomycin complex. The secondary structure nomenclature is based on that of *E. coli* DXR (EcDXR)[16]. The subunit of PfDXR consists of two large domains separated by a cleft containing a deep pocket, a linker region, and a small C-terminal domain (Fig. 2a). One of the large domains is responsible for NADPH binding, and the other provides the groups necessary for catalysis (metal and substrate binding). The two large domains are similar in size; the NADPH-binding domain is somewhat larger and comprises 154 residues, whereas the catalytic domain comprises 139 residues.

The NADPH-binding domain comprises residues 77 to 230 (Fig. 2a, blue). The basic element of the secondary structure of this domain is a seven-stranded β-sheet in the centre of the domain that is sandwiched by two arrays of three α-helices. The six-stranded parallel β-sheet flanked by four α-helices constitutes a characteristic dinucleotide-binding motif, or Rossmann fold, composed of two βαβαβ units (β1α1β2α2β3 and β5α5β6α6β7). The NADPH-binding domain of PfDXR differs from the classic Rossmann fold in that an additional αβ motif (α3β4) is inserted after β3. An NADPH molecule is found in a crevice of the NADPH-binding domain of each of the two crystallographically independent subunits in an asymmetric unit

of the PfDXR crystal. The binding mode of the NADPH molecule is quite similar to that observed for EcDXR[16].

The catalytic domain comprises residues 231 to 369 (Fig. 2a, green). It is an α/β-type structure consisting of five α-helices



a

b

c
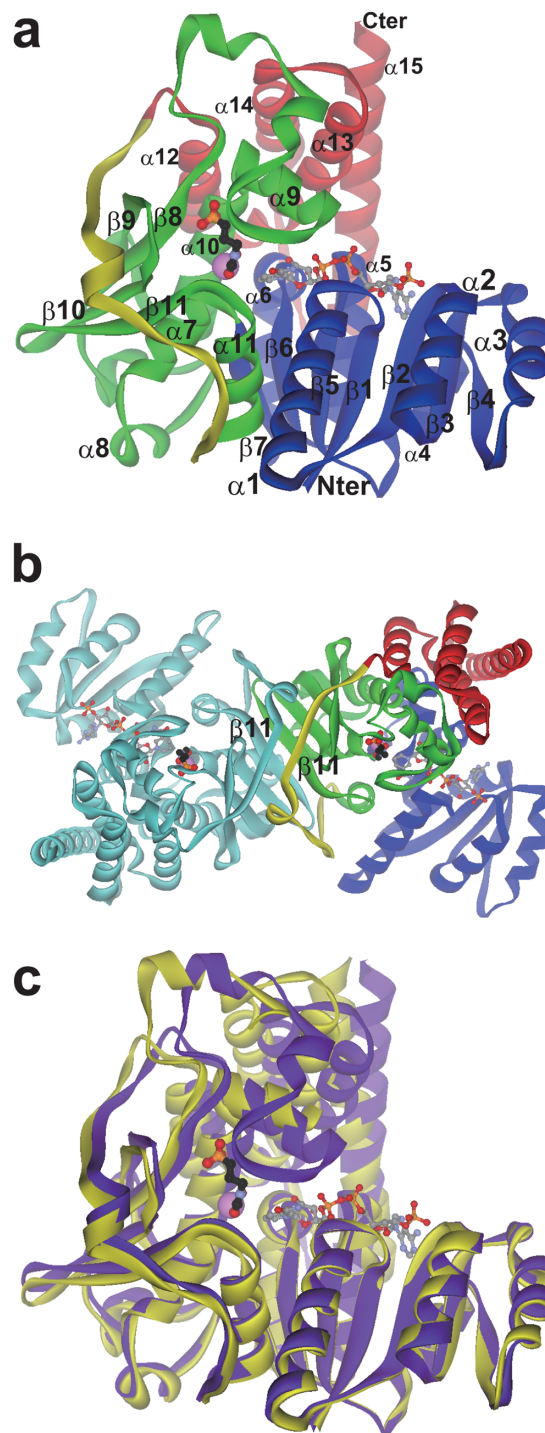
Figure 2 | **The three-dimensional structure of PfDXR.** **a,** The subunit structure of the fosmidomycin-bound quaternary complex of PfDXR. The NADPH-binding, catalytic, linker, and C-terminal domains are depicted in blue, green, yellow, and red, respectively. The bound fosmidomycin (black for carbon) and NADPH (gray for carbon) molecules are shown as ball-and-stick models. **b,** The overall structure of PfDXR. One subunit is coloured as in **a**. The other subunit is coloured cyan. **c,** Comparison of the crystal structure of the inhibitor-free ternary complex of PfDXR (yellow) and that of the inhibitor (fosmidomycin)-bound quaternary complex of PfDXR (purple).
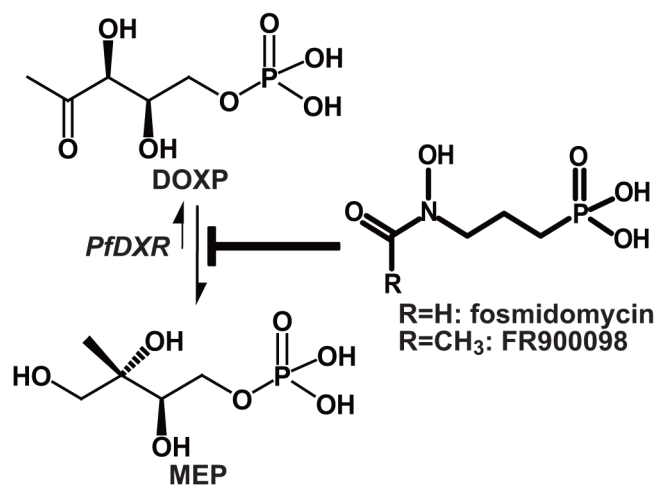


Figure 1 | **The structures of substrate, product, and inhibitors of PfDXR.**

($\alpha7$–$\alpha11$) and four $\beta$-strands ($\beta8$–$\beta11$). The domain's structural core is an open-faced, four-stranded $\beta$-sheet with one parallel and two antiparallel alignments. The loops and helices cover only one side of the $\beta$-sheet. The bound metal ion is found in the bottom of a crevice in the catalytic domain. The inhibitor molecule, fosmidomycin (or FR900098), is also found in the crevice of the catalytic domain in the inhibitor-bound quaternary complex. The binding mode of the inhibitor molecules will be presented later.

The C-terminal domain comprises residues 396 to 486 (Fig. 2a, red). This domain is composed of a four-helix bundle structure ($\alpha12$–$\alpha15$). The linker region comprises residues 370 to 395 (Fig. 2a, yellow). This region connects the catalytic domain to the C-terminal domain, spanning the open face of the catalytic domain.

In the present crystal form, two subunits of an asymmetric unit formed a homodimer (Fig. 2b), which has also been observed in the crystal structures of DXRs from other species[16–23]. Intersubunit interactions in PfDXR occur primarily along strands of the catalytic domain $\beta11$, thus forming an eight-stranded $\beta$-sheet from the four-stranded $\beta$-sheet in the catalytic domains of each subunit. The linker region also contributes to dimer formation by interacting with the same region of the other subunit (the antiparallel $\beta$-sheet-like structure formed by Ser387 to Phe391). The NADPH-binding domains and C-terminal domains of each subunit are located far from the core of the dimer, and they have minimal interaction with each other. The NADPH-binding and C-terminal domains therefore appear to be more mobile than the catalytic domains that form the structural core of the dimer.

A comparison of the crystal structure of the inhibitor-free ternary complex of PfDXR with those of the inhibitor (fosmidomycin or FR900098)-bound quaternary complexes of PfDXR showed that the large cleft between the NADPH-binding and catalytic domains were closed upon inhibitor binding (Fig. 2c). A closed conformation was observed for both crystallographically independent subunits of the inhibitor-bound quaternary complexes. In addition, the disordered loop region in the inhibitor-free form (residues 291 to 299) was well defined in the inhibitor-bound quaternary complexes. It has been reported that the known DXR structures can be categorised into three types of conformations: an open form with the flexible loop opened (without inhibitor), an open form with the flexible loop closed (with inhibitor, prepared by soaking), and a closed form with the flexible loop closed (with inhibitor, prepared by co-crystallisation)[23]. The crystal structures of the inhibitor-bound quaternary complexes of PfDXR correspond to the third type and represent the first example of a complete closed form with the flexible loop closed, in that all the components (enzyme-NADPH-metal-inhibitor) were identified in both subunits of the dimeric DXR molecule.

**Fosmidomycin complex.** The fosmidomycin molecule lies in a crevice of the catalytic domain (Figs. 2, 3a and 3b). The fosmidomycin-binding cavity consists of three regions: a binding pocket for the phosphonate moiety of fosmidomycin, a hydrophobic patch for the carbon backbone of the inhibitor, and a binding pocket for the hydroxamate group of the inhibitor. The phosphonate group of fosmidomycin forms a tightly hydrogen-bound network with Ser270, Asn311, two water molecules, and His293, which is disordered in the inhibitor-free form. The carbon backbone of the inhibitor lies parallel to the indole ring of Trp296 (Fig. 3a). The backbone also interacts with Met298. These hydrophobic residues are disordered in the inhibitor-free form and constitute a hydrophobic patch in the fosmidomycin complex.

The hydroxamate group coordinates a $Mg^{2+}$ ion that is bound by residues Asp231, Glu233, and Glu315. The side chain of Lys312 is involved in stabilising the side chains of Glu233 and Glu315. The $Mg^{2+}$ ion in the inhibitor complex has a distorted trigonal bipyramidal geometry and binds to three protein ligands and two inhibitor atoms (Figs. 3a and 3c). The side chains of Asp231(OD1) and Glu233(OE1), as well as the N-hydroxyl oxygen of fosmidomycin(O2), are the equatorial ligands, and the axial ligands are the side chain of Glu315(OE2) and the N-formyl oxygen of fosmidomycin(O1). Consequently, two oxygen atoms of the hydroxamate group of the bound inhibitor adopt a cis arrangement. Although a few DXR structures that complex with fosmidomycin have been reported[18–20,22,23], the metal coordination geometry observed in the present fosmidomycin complex is consistent only with subunit A of the quaternary (NADPH-$Mn^{2+}$-fosmidomycin) complex of M. tuberculosis DXR (MtDXR)[22], in which the electron density of all components was clearly identified in the active site of one subunit of the dimer, although the active site of the other subunit was empty. The crystal packing effect of MtDXR probably prevented the formation of a symmetrical dimer. The failure of the EcDXR and TmDXR structures[18–20,23] to form well-ordered quaternary complexes could be due to unfavourable crystallisation conditions (acidic pH) for the binding of the active site metal ion, as the crystals of PfDXR and MtDXR were obtained at weak basic conditions suitable for metal binding.

**FR900098 complex.** In the present crystal structure analysis, we also successfully determined the FR900098-bound quaternary complex structure (Figs. 3b and 3d). This is the first crystal structure analysis of DXR complexed with FR900098, the most potent DXR inhibitor available. The structure of FR900098 indicates that it is a closely related derivative of fosmidomycin, and it is approximately twice as active as fosmidomycin against cultured parasites and in animal models[5]. The structural difference between the inhibitors is the replacement of the formyl hydrogen of fosmidomycin with a methyl group in FR900098 (Fig. 1). The overall structure and the interactions of the inhibitor with the metal and the enzyme are similar to those observed in the fosmidomycin-bound quaternary complex. The methyl group of FR900098 is in van der Waals contact with the side chain of Trp296 and is structurally equivalent to the C1 of the DOXP substrate (Fig. 1). The preferred hydrophobic interaction between the methyl group of FR900098 and the indole ring of Trp296 can explain the increased activity against PfDXR of FR900098 compared with fosmidomycin[5,24]. Alternatively, this interaction might be important for establishing the cis arrangement of the two oxygen atoms of the hydroxamate group, in which six atoms (C-N(-O)-C(=O)-C) are in the same plane as the resonance structures (Figs. 3c and 3d), allowing them to bind to the active site metal ion. By comparing the structures of the FR900098 and fosmidomycin complexes, an induced fit movement of the active site residues of PfDXR to accommodate the unique methyl group of FR900098 was suggested for the FR900098 complex (Fig. 3d). Particularly noteworthy is the approximately $10°$ rotation of the $\chi_2$ angle of the indole ring of Trp296. A multiple sequence alignment of the flexible loop region of DXR (residues 291 to 299 in PfDXR) from various organisms (Fig. 3e) shows that the buried residues (His293, Trp296, and Met298 in PfDXR) in the inhibitor-bound structure are completely conserved, whereas the exposed residues are not well conserved, except for Pro294 in PfDXR, which may be important for maintaining the structure of the flexible loop. This multiple sequence alignment indicates the important role of these buried residues in the inhibitor/substrate binding associated with loop closure. It should also be noted that Gly299 in PfDXR is conserved. The Gly residue may contribute to the flexibility of the flexible loop as an active site flap.

## Discussion

On the basis of the present crystal structure analyses, the structure-activity relationship studies of fosmidomycin and its analogues against EcDXR or the in vitro growth inhibition of P. falciparum[24–32] can be re-evaluated with respect to the three moieties of fosmidomycin
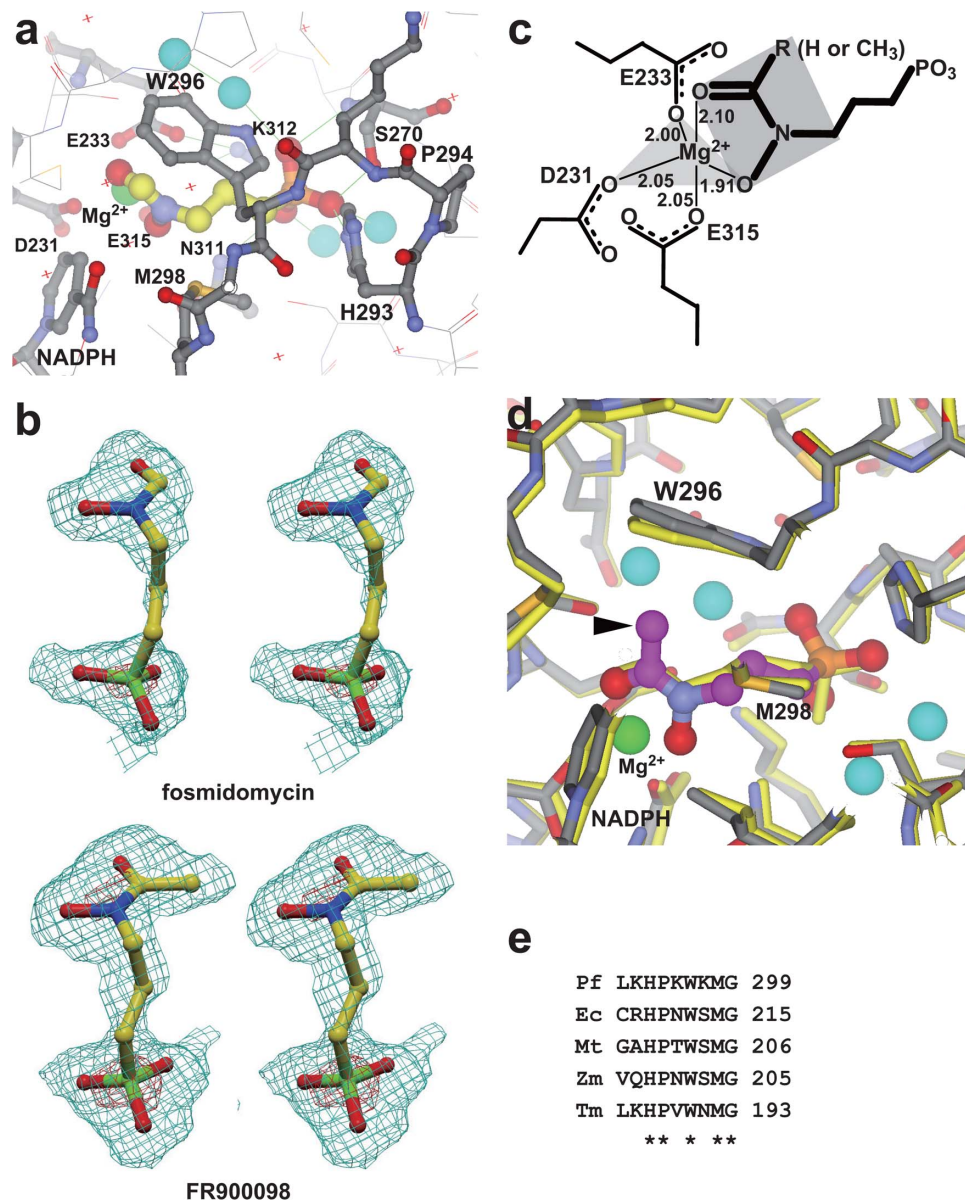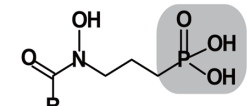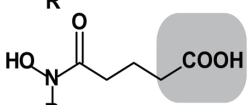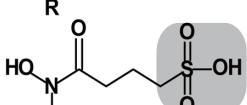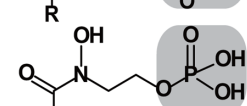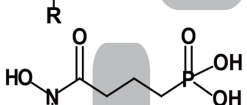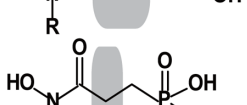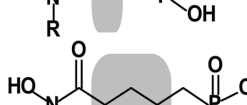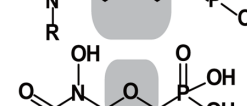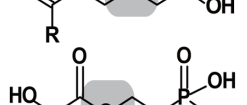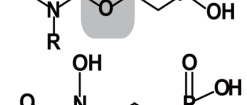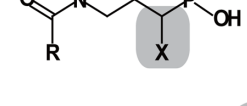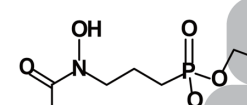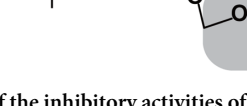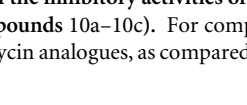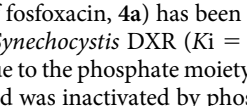
**Figure 3 | The inhibitor-binding sites of the quaternary complexes of PfDXR.** a, Fosmidomycin complex. The carbon atoms of fosmidomycin, the four buried water molecules, and the bound Mg²⁺ ion are shown in yellow, cyan, and green, respectively. b, Stereo diagrams showing the |Fo| − |Fc| omit maps of bound inhibitors in fosmidomycin (top) and FR900098 (bottom) complexes at 1.8- and 2.15-Å resolutions, respectively. To exclude a model bias, the structures were refined in the absence of the inhibitor molecules before the map calculation. The amplitude |Fc| and the phase angle calculated from the partial structure were then used to calculate the |Fo| − |Fc| omit map. The contour levels are 2.5 σ (cyan) and 10.0 σ(red). c, Schematic drawing of the metal coordination system observed in the quaternary complexes of PfDXR. Bond lengths are shown in Å. d, FR900098 complex. The carbon atoms of the FR900098 molecule are shown in magenta. To compare the induced-fit movement of the active site residues upon inhibitor binding, LSQ fitting was performed with respect to the 11 atoms common to the inhibitors in the fosmidomycin and FR900098 complexes. The RMSD for the 11 pairs was 0.50 Å. The methyl group of the bound FR900098 molecule is indicated by an arrow head. The fo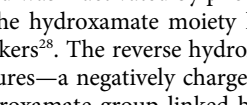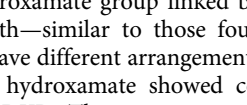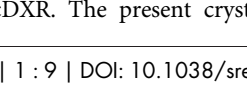smidomycin complex is shown in yellow stick models. e, Multiple sequence alignment of the flexible loop region of DXRs. The abbreviations (GenBank accession numbers) are as follows: Pf (AAD03739), *Plasmodium falciparum* DXR; Ec (BAA77848), *Escherichia coli* DXR; Mt (CAA98375), *Mycobacterium tuberculosis* DXR; Zm (AAD29659), *Zymomonas mobilis* DXR; Tm (AAD35970), *Thermotoga maritima* DXR. The residue numbers are shown on the right.

(compound **1a** in Fig. 4): the phosphonate group, the carbon backbone, and the hydroxamate group. Most reported efforts at synthesising fosmidomycin analogues involve modifications of the phosphate and hydroxamate moieties.

Replacement of a phosphonate group by other isosteric groups, such as a carboxylate (**2a** and **2b**) or a sulphonate (**3a** and **3b**), was evaluated for reverse hydroxamate analogues of fosmidomycin[26]. The results showed drastically decreased inhibitory activity against EcDXR and suggest that the tight hydrogen bond network around the phosphonate group of fosmidomycin or FR900098 revealed

by the present crystal structure analysis is essential for inhibitor binding. The failure of the carboxylate analogue to inhibit EcDXR can be explained by a structural difference: a phosphonate has a pyramidal structure, and a carboxylate has a planar structure. The failure of the sulphonate analogue to inhibit EcDXR is not as clear as in the case of a carboxylate analogue. The difference between the phosphonate and sulphonate groups is that the C-P and P-O bond lengths are shorter than those of the C-S and S-O bonds. This difference might prevent the sulphonate group from ideal binding. On the other hand, the phosphate analogue of FR900098 (**4b**) (the

**Figure 4 | Summary of the inhibitory activities of fosmidomycin analogues against EcDXR and *in vitro* growth inhibition of *P. falciparum* strain 3D7 (or strain K1 for compounds 10a–10c).** For compounds **4a** and **4b**, the relative $K_i$ values against *Synechocystis* DXR are shown. The relative inhibitory activities of fosmidomycin analogues, as compared with fosmidomycin, are shown as "+++" (> 10), "++" (1 - 10), "+" (1/10 - 1), and "−" (< 1/10).

*N*-acetyl analogue of fosfoxacin, **4a**) has been reported to be a more potent inhibitor of *Synechocystis* DXR ($K_i$ = 2 nM) than fosmidomycin[27]; however, due to the phosphate moiety in its structure, it was prone to cleavage and was inactivated by phosphatases *in vivo*.

Modification of the hydroxamate moiety has been reported by Rohmer and co-workers[28]. The reverse hydroxamate analogues (**5a** and **5b**) exhibit features—a negatively charged phosphonate group and a chelating hydroxamate group linked by a carbon backbone with the same length—similar to those found in fosmidomycin and FR900098 but have different arrangements in the hydroxamate group. The reverse hydroxamate showed comparable inhibitory activities against EcDXR. The present crystal structure analyses

revealed that the *cis* arrangements of the two oxygen atoms of the hydroxamate group are necessary for the metal coordination of the inhibitors. The reverse hydroxamate analogues could bind to the enzyme active site with similar conformations. Alternatively, another functional group containing *cis* oxygen atoms (not only the functional grops of hydroxamate or reverse hydroxamate) might have comparable metal coordination ability.

There have been few reports of modification of the length of the carbon backbone between the hydroxamate moiety and the phosphonate. Attempts to shorten the two-methylene spacer for reverse hydroxamate analogues of fosmidomycin resulted in drastically decreased inhibitory activity against EcDXR (**6a** and **6b**), whereas

lengthening the spacer resulted in moderately decreased activity (**7a** and **7b**)[26]. The present crystal structures revealed extended conformations of the bound inhibitors. Shorter compounds were too short to occupy both the phosphonate binding site and the hydroxamate binding site. The long spacer of longer compounds prevented them from efficiently binding to the active site.

The introduction of an electron withdrawing group to the carbon backbones of fosmidomycin and FR900098 or their reverse hydroxamate analogues was recently reported[29–31]. A β-oxa modification yielded derivatives (**8a** and **8b**) with higher activity against the *P. falciparum* 3D7 strain than fosmidomycin, whereas a γ-oxa modification of reverse hydroxamate analogues resulted in less-active derivatives (**9a** and **9b**)[29]. The present crystal structure analyses revealed only a hydrophobic interaction between the carbon backbone of the inhibitors and Trp296, indicating that the introduction of an oxygen atom to the carbon backbone is not advantageous for hydrogen bonding to the active site of PfDXR. Instead, the introduction of an electronegative oxygen atom might decrease the p$K_{a2}$ of the phosphonate group. Thus, the phosphonate group could form a doubly ionised form, which is more favourable for binding. For the same reason, an α-aryl substituted fosmidomycin (**10a**)[30] and α-halogenated analogues of FR900098 (**10b** and **10c**)[31] showed higher potency than the reference compounds. Because the carbon atom at the α-position of fosmidomycin or FR900098 points towards His293 and Met298 on the side chains belonging to the flexible loop at the active site (Fig. 3a), an α-substituted halogen atom (**10b** and **10c**) could be accommodated by a slight induced fit movement of the flexible loop. However, a bulky functional group in the α-position of **compound 10a** appears to be too large to bind; a large-scale induced fit movement of the enzyme active site would be necessary to accommodate the bulky inhibitor. Alternatively, the aromatic ring of the bulky inhibitor may improve the ability of the inhibitor to cross the parasitic cell membrane.

To develop new PfDXR inhibitors that have higher inhibitory activity against the proliferation of *P. falciparum*, we must consider two aspects of inhibitors. One is the improvement of the direct interactions between the bound inhibitor and PfDXR, and the other is refinement of the pharmacokinetic profile of inhibitors for clinical use.

With respect to the former issue, analysis of the active sites of present quaternary complexes revealed the presence of buried and conserved water molecules in the vicinity of the phosphonate group of the inhibitors (Figs. 3a and 3c). This finding indicates that the active site is able to accommodate small functional groups attached to the phosphonate group. Our prediction is consistent with that for EcDXR[32]. Interestingly, however, it has been reported that bulky monoesters (phenyl ethyl and 1- or 2-naphthyl ethyl) showed significant activity against cultured malaria parasites[32]. This unexpected observation is not explained by the present crystal structures because the space at the buried active site is too small to accommodate such bulky groups if the closed conformation observed in the present crystal structure analyses is regarded as rigid. One explanation could be that the real target of these compounds is another protein essential for the survival of *P. falciparum*. If not, we must assume that PfDXR can accommodate a larger functional group attached to the basic skeleton of fosmidomycin in the active site, as in the case of the binding of the slightly larger FR900098 by a relatively large-scale induced fit mechanism. Interdomain flexibility and the existence of the flexible loop of PfDXR, revealed by the present crystal structure analyses, would enable this mechanism.

In addition to the efforts to improve the binding affinity of fosmidomycin to PfDXR, refinement of its pharmacokinetic profile would be required for clinical use. Fosmidomycin alone or in combination with clindamycin shows incomplete eradication of the infection[33]. The eradication rate is expected to rise when the half-life and bioavailability are improved. With respect to the pharmacokinetic

profiles of fosmidomycin and FR900098, repeated high doses are required to achieve acceptable cure rates[13–15] because it has been reported that the oral bioavailabilities of these compounds are relatively poor, with a resorption rate of approximately 30% in rats[34]. This is due to the low lipophilicity of these compounds as a result of high ionisation of the phosphonate moiety at physiological pH. To overcome this disadvantage, prodrug approaches were taken that used bio labile ester moieties that mask the polar phosphonate moiety of the inhibitors, and promising results were reported (e.g., an $IC_{50}$ value for *in vitro* growth inhibition of *P. falciparum* at the sub-µM level for **compound 11**)[29]. Because the bis(pivaloyloxymethyl)ester moiety is removed by an esterase *in vivo*, the binding mode of **compound 11** would be essentially the same as that of FR900098 presented here.

Here, we analysed the fosmidomycin and FR900098-bound quaternary complexes of PfDXR. Our study revealed that (i) an intrinsic flexibility of the PfDXR molecule accounts for the induced-fit movement that accommodates the bound inhibitor in the active site, and (ii) a *cis* arrangement of the oxygen atoms of the hydroxamate group of the bound inhibitor is essential for tight binding of the inhibitor to the active site metal. To develop new PfDXR inhibitors with desirable pharmacokinetic profiles, both (i) a structure-based inhibitor design using the present quaternary complex structures as a guide and (ii) a prodrug approach that masks the polar phosphonate group should be considered. We believe that our study will serve as a useful guide for the development of more potent PfDXR inhibitors.

## Methods

**Overexpression and purification.** Expression and purification of PfDXR were performed as previously described[35]. Because the first 30 amino acids of PfDXR resemble an endoplasmic reticulum signal sequence, and the following 44 amino acids exhibit the characteristics of a plastidial targeting sequence, the DNA-encoding residues from Lys75 to Ser488 (C-terminus) of PfDXR were obtained by reverse-transcription PCR with total RNA from *P. falciparum* (FCR-3) as the template. The target DNA was PCR-amplified and cloned into a pQE30 expression plasmid (QIAGEN). *E. coli* BL21(DE3) cells harbouring the expression plasmid were grown in LB media at 310 K to an $OD_{600}$ of 0.6. Overexpression of PfDXR was induced by 0.5 mM IPTG for 20 h at 293 K. After this period, cells were harvested by centrifugation at 8,000 *g* and disrupted using ultrasonication on ice. The cell extract was obtained by centrifugation at 15,000 *g* and was applied to a 1-ml HisTrap HP column. PfDXR was eluted with 0.5 M imidazole solution. The PfDXR was further purified by gel chromatography using a Superdex 200 pg column. The fractions containing PfDXR were pooled and concentrated to 10 mg/ml using a Centricon-30 microconcentrator (Millipore).

**Crystallisation.** To obtain the ternary (PfDXR-NADPH-Mn[2]) complex, the protein solution (10 mg/ml PfDXR, 50 mM Tris-HCl pH 7.8, and 2 mM DTT) was mixed with cofactor solution (50 mM Tris-HCl pH 7.8, 2 mM DTT, 6 mM NADPH, and 4 mM MnCl₂) at a volume ratio of 1 : 1. Crystallisation was performed by the hanging-drop method, in which 2 µl of protein solution (5 mg/ml PfDXR, 3 mM NADPH, and 2 mM Mn^{2+}) was mixed with the same volume of reservoir solution (0.1 M Tris-HCl pH 8.0, 20% (w/v) PEG3350, and 0.3 M NaCl) and incubated at 293 K. The drops were suspended over 500 µl of reservoir solution in 24-well plates. To obtain the quaternary (PfDXR-NADPH-Mg^{2+}-fosmidomycin or FR900098) complexes, the protein solution was mixed with inhibitor solution (50 mM Tris-HCl pH 7.8, 2 mM DTT, 6 mM NADPH, 4 mM MgCl₂, and 4 mM fosmidomycin or FR900098) at a volume ratio of 1 : 1. Crystallisation was performed using the hanging-drop method, in which 2 µl of protein solution (5 mg/ml PfDXR, 3 mM NADPH, 2 mM Mg^{2+}, and 2 mM fosmidomycin or FR900098) was mixed with the same volume of reservoir solution (0.1 M Tris-HCl pH 8.0, 20% (w/v) PEG8000, and 0.3 M calcium acetate) and incubated at 293 K. The drops were suspended over 500 µl of reservoir solution in 24-well plates.

**X-ray data collection.** For data collection under cryogenic conditions, the ternary complex crystals in a droplet were directly transferred to the harvesting solution (3 mM NADPH, 2 mM Mn^{2+}, 0.3 M NaCl, 20% (w/v) PEG3350, and 20% (v/v) glycerol in 0.1 M Tris-HCl pH 8.0) for 1 min. The quaternary complex crystals in a droplet were transferred directly to a cryoprotectant, Paratone-N (Hampton Research). The crystals were mounted in nylon loops and flash-cooled in a cold nitrogen-gas stream at 100 K just prior to data collection. Data were collected by the rotation method at 100 K using an ADSC Q270 CCD detector with synchrotron radiation (λ = 1.000 Å on beamline 17A of the Photon Factory (PF), Tsukuba, Japan) for the ternary complex and using an ADSC Q210r CCD detector with synchrotron radiation (λ = 1.000 Å on beamline NW12A of the PF-AR) for the quaternary complexes. The Laue group and unit-cell parameters were determined using the

HKL2000 package. Cell parameters and data-collection statistics are summarised in Table S1.

**Structure determination.** Initial phase determination was performed for the ternary complex of PfDXR by molecular replacement (MR) using the coordinate set of the *E. coli* DXR dimer (PDB code 1ONN), which shares approximately 30% of its amino acid sequence identity with PfDXR, as a search model. The phase determination was performed using the AMoRe program[36] from the CCP4 suite[37]. Automatic model building and refinement were performed using the ARP/wARP[38] and REFMAC5[39] programs, and further iterative manual model building and refinement at 1.86 Å resolution was performed with the XtalView[40] and REFMAC5 programs. The refined ternary complex model was used for structure determination of the quaternary (fosmidomycin) complex of PfDXR by the MR method, which was performed using procedures similar to those described above. The fosmidomycin complex of PfDXR was refined at a 1.9-Å resolution. The refined fosmidomycin complex model was then used as a template for the structure refinement of the quaternary (FR900098) complex of PfDXR by the D-Fourier method because the crystals of these quaternary complexes were isomorphous to each other. The FR900098 complex of PfDXR was refined at a 2.15-Å resolution. Refinement statistics for the ternary and quaternary complexes of PfDXR are summarised in Table S1. Figures 2a, 2b, 2c, 3a, and 3d were produced with the DS ViewerPro program (Accelrys, Inc.). Figure 3b was produced with the XtalView and Raster3D[41] programs. Least-squares comparisons of the molecular models were performed using the XtalView program.

1.  Snow, R.W., Guerra, C.A., Noor, A.M., Myint, H.Y. & Hay, S.I. The global distribution of clinical episodes of *Plasmodium falciparum* malaria. *Nature* **434**, 214–217 (2005).

2.  Winzeler, E.A. Malaria research in the post-genomic era. *Nature* **455**, 751–756 (2008).

3.  Rohmer, M. The discovery of a mevalonate-independent pathway for isoprenoid biosynthesis in bacteria, algae, and higher plants. *Nat. Prod. Rep.* **16**, 565–574 (1999).

4.  Lichtenthaler, H.K. Sterols and isoprenoids. *Biochem. Soc. Trans.* **28**, 785–789 (2000).

5.  Jomaa, H., Wiesner, J., Sanderbrand, S., Altincicek, B., Weidemeyer, C., Hintz, M., Turbachova, I., Eberl, M., Zeidler, J., Lichtenthaler, H.K., Soldati, D. & Beck, E. Inhibitors of the nonmevalonate pathway of isoprenoid biosynthesis as antimalarial drugs. *Science* **285**, 1573–1576 (1999).

6.  Kuzuyama, T., Takahashi, S. & Seto, H. Construction and characterization of *Escherichia coli* disruptants defective in the *yaeM* gene. *Biosci. Biotechnol. Biochem.* **63**, 776–778 (1999).

7.  Julsing, M.K., Rijpkema, M., Woerdenbag, H.J., Quax, W.J. & Kayser, O. Functional analysis of genes involved in the biosynthesis of isoprene in *Bacillus subtilis*. *Appl. Microbial. Biotechnol.* **75**, 1377–1384 (2007).

8.  Brown, A.C., Eberl, M., Crick, D.C., Jomaa, H. & Parish, T. The nonmevalonate pathway of isoprenoid biosynthesis in *Mycobacterium tuberculosis* is essential and transcriptionally regulated by Dxs. *J. Bacteriol.* **192**, 2424–2433 (2010).

9.  Odom, A.R. & Van Voorhis, W.C. Functional genetic analysis of the *Plasmodium falciparum* deoxyxylulose 5-phosphate reductoisomerase gene. *Mol. Biochem. Parasitol.* **170**, 108–111 (2010).

10. Takahashi, S., Kuzuyama, T., Watanabe, H. & Seto, H. A 1-deoxy-D-xylulose 5-phosphate reductoisomerase catalyzing the formation of 2-C-methyl-D-erythritol 4-phosphate in an alternative nonmevalonate pathway for terpenoid biosynthesis. *Proc. Natl. Acad. Sci. USA* **95**, 9879–9884 (1998).

11. Proteau, P.J. 1-deoxy-D-xylulose 5-phosphate reductoisomerase: an overview. *Bioorg. Chem.* **32**, 483–493 (2004).

12. Kuzuyama, T., Shimizu, T., Takahashi, S. & Seto, H. Fosmidomycin, a specific inhibitor of 1-deoxy-D-xylulose 5-phosphate reductoisomerase in the nonmevalonate pathway for terpenoid biosynthesis. *Tetrahedron Lett.* **39**, 7913–7916 (1998).

13. Missinou, M.A., Borrmann, S., Shindler, A., Issifou, S., Adegnika, A.A., Matsiegui, P.-B., Binder, R., Lell, B., Wiesner, J., Baranek, T., Jomaa, H. & Kremsner, P.G. Fosmidomycin for malaria. *Lancet* **360**, 1941–1942 (2002).

14. Lell, B., Ruangweerayut, R., Wiesner, J., Missinou, M.A., Shindler, A., Baranek, T., Hintz, M., Hutchinson, D., Jomaa, H. & Kremsner, P.G. Fosmidomycin, a novel chemotherapeutic agent for malaria. *Antimicrob. Agents Chem.* **47**, 735–738 (2003).

15. Borrmann, S., Issifou, S., Esser, G., Adegnika, A.A., Ramharter, M., Matsiegui, P.-B., Oyakhirome, S., Mawili-Mboumba, D.P., Missinou, M.A., Kun, J.F.J., Jomaa, H. & Kremsner, P.G. Fosmidomycin-clindamycin for the treatment of *Plasmodium falciparum* malaria. *J. Infect. Dis.* **190**, 1534–1540 (2004).

16. Reuter, K., Sanderbrand, S., Jomaa, H., Wiesner, J., Steinbrecher, I., Beck, E., Hintz, M., Klebe, G. & Stubbs, M.T. Crystal structure of 1-deoxy-D-xylulose 5-phosphate reductoisomerase, a crucial enzyme in the non-mevalonate pathway of isoprenoid biosynthesis. *J. Biol. Chem.* **277**, 5378–5384 (2002).

17. Yajima, S., Nonaka, T., Kuzuyama, T., Seto, H. & Ohsawa, K. Crystal structure of 1-deoxy-D-xylulose 5-phosphate reductoisomerase complexed with cofactors: Implications of a flexible loop movement upon substrate binding. *J. Biochem.* **131**, 313–317 (2002).

18. Steinbacher, S., Kaiser, J., Eisenreich, W., Huber, R., Bacher, A. & Rohdich, F. Structural basis of fosmidomycin action revealed by the complex with 2-C-methyl-D-erythritol 4-phosphate synthase (IspC). *J. Biol. Chem.* **278**, 18401–18407 (2003).

19. MacSweeney, A., Lange, R., Fernandes, R.P.M., Shultz, H., Dale, G.E., Douangamath, A., Proteau, P.J. & Oefner, C. Crystal structure of *E. coli* 1-deoxy-D-xylulose 5-phosphate reductoisomerase in a ternary complex with the antimalarial compound fosmidomycin and NADPH reveals a tight-binding closed enzyme conformation. *J. Mol. Biol.* **345**, 115–127 (2005).

20. Yajima, S., Hara, K., Iino, D., Sasaki, Y., Kuzuyama, T., Ohsawa, K. & Seto, H. Structure of 1-deoxy-D-xylulose 5-phosphate reductoisomerase in a quaternary complex with a magnesium ion, NADPH and the antimalarial drug fosmidomycin. *Acta Crystallogr F***63**, 466–470 (2007).

21. Ricagno, S., Grolle, S., Bringer-Meyer, S., Sahm, H., Lindqvist, Y. & Schneider, G. Crystal structure of 1-deoxy-D-xylulose 5-phosphate reductoisomerase from *Zymomonas mobilis* at 1.9-Å resolution. *Biochim. Biophys. Acta* **1698**, 37–44 (2004).

22. Henriksson, L.M., Unge, T., Carlsson, J., Aqvist, J., Mowbray, S.L. & Jones, T.A. Structures of *Mycobacterium tuberculosis* 1-deoxy-D-xylulose 5-phosphate reductoisomerase provide new insight into catalysis. *J. Biol. Chem.* **282**, 19905–19916 (2007).

23. Takenoya, M., Ohtaki, A., Noguchi, K., Endo, K., Sasaki, Y., Ohsawa, K., Yajima, S. & Yohda, M. Crystal structure of 1-deoxy-D-xylulose 5-phosphate reductoisomerase from the hyperthermophile *Thermotoga maritima* for insights into the coordination of conformational changes and an inhibitor binding. *J. Struct. Biol.* **170**, 532–539 (2010).

24. Giessmann, D., Heidler, P., Haemers, T., Van Calenbergh, S., Reichenberg, A., Jomaa, H., Weidemeyer, C., Sanderbrand, S., Wiesner, J. & Link, A. Towards new antimalarial drugs: synthesis of non-hydrolyzable phosphate mimics as feed for a predictive QSAR study on 1-deoxy-D-xylulose-5-phosphate reductoisomerase inhibitors. *Chem. Biodivers.* **5**, 643–656 (2008).

25. Singh, N., Cheve, G., Avery, M. A. & McCurdy, C. R. Targeting the methyl erythritol phosphate (MEP) pathway for novel antimalarial, antibacterial and herbicidal drug discovery: inhibition of 1-deoxy-D-xylulose-5-phosphate reductoisomerase (DXR) enzyme. *Curr. Pharm. Des.* **13**, 1161–1177 (2007).

26. Zingle, C., Kuntz, L., Tritsch, D., Grosdemange-Billiard, C. & Rohmer, M. Isoprenoid biosynthesis via the methylerythritol phosphate pathway: structural variations around phosphonate anchor and spacer of fosmidomycin, a potent inhibitor of deoxyxylulose phosphate reductoisomerase. *J. Org. Chem.* **75**, 3203–3207 (2010).

27. Woo, Y.-H., Fernandes, R. P. M. & Proteau, P. J. Evaluation of fosmidomycin analogs as inhibitors of the *Synechocystis* sp. PCC6803 1-deoxy-D-xylulose-5-phosphate reductoisomerase.*Bioorg. Med.Chem.* **14**, 2375–2385 (2006).

28. Kuntz, L., Tritsch, D., Grosdemange-Billiard, C., Hemmerlin, A., Willem, A., Bach, T. J., & Rohmer, M. Isoprenoid biosynthesis as a target for antibacterial and antiparasitic drugs: phosphonohydroxamic acids as inhibitors of deoxyxylulose phosphate reducto-isomerase. *Biochem. J.* **386**, 127–135 (2005).

29. Haemers, T., Wiesner, J., Giessmann, D., Verbrugghen, T., Hillaert, U., Ortmann, R., Jomaa, H., Link, A., Schlitzer, M. & Van Calenbergh, S. Synthesis of β- and γ-oxa isosteres of fodmidomycin and FR900098 as antimalarial candidates. *Bioorg. Med. Chem.* **16**, 3361–3371 (2008).

30. Haemers, T., Wiesner, J., Van Poecke, S., Goeman, J., Henschker, D., Beck, E., Jomaa, H. & Van Calenbergh, S. Synthesis of α-substituted fosmidomycin analogues as highly potent Plasmodium falciparum growth inhibitors. *Bioorg. Med. Chem. Lett.* **16**, 1888–1891 (2006).

31. Verbrugghen, T., Cos, P., Maes, L. & Van Calenbergh, S. Synthesis and evaluation of α-halogenated analogues of 3-(acetylhydroxyamino)propylphosphonic acid (FR900098) as antimalarials. *J. Med. Chem.* **53**, 5342–5346 (2010).

32. Perruchon, J., Ortmann, R., Altenkamper, M., Silber, K., Weisner, J., Jomaa, H., Klebe, G. & Schlitzer, M. Studies addressing the importance of charge in the binding of fosmidomycin-like molecules to deoxyxylulosephosphate reductoisomerase. *Chem. Med. Chem.* **3**, 1232–1241 (2008).

33. Borrmann, S., Lundgren, I., Oyakhirome, S., Oyakhirome, S., Impouma, B., Matsiegui, P.-B., Adegnika, A.A., Issifou, S., Kun, J.F.J., Hutchinson, D., Wiesner, J., Jomaa, H. & Kremsner, P.G. Fosmidomycin plus clindamycin for treatment of pediatric patients aged 1 to 14 years with *Plasmodium falciparum* malaria. *Antimicrob. Agents Chemother.* **50**, 2713–2718 (2006).

34. Tsuchiya, T., Ishibashi, K., Terakawa, M., Nishiyama, M., Itoh, N. & Noguchi, H. Pharmacokinetics and metabolism of fosmidomycin, a new phosphonic acid, in rats and dogs. *Eur. J. Drug Metab. Pharmacokinet.* **7**, 59–64 (1982).

35. Umeda, T., Tanaka, N., Kusakabe, Y., Nakanishi, M., Kitade, Y. & Nakamura, K.T. Crystallization and preliminary X-ray crystallographic study of 1-deoxy-D-xylulose 5-phosphate reductoisomerase from *Plasmodium falciparum*. *Acta Crystallogr. F***66**, 330–332 (2010).

36. Navaza, J. AMoRe: an automated program for molecular replacement. *Acta Crystallogr. A***50**, 157–163 (1994).

37. Collaborative computational project, number 4. The CCP4 suite: programs for protein crystallography. *Acta Crystallogr. D***50**, 760–763 (1994).

38. Lamzin, V.S. & Wilson, K.S. Automated refinement of protein models. *Acta Crystallogr. D***49**, 129–147 (1993).

39. Murshudov, G.N., Vagin, A.A. & Dodson, E.J. Refinement of macromolecular structures by the maximum-likelihood method. *Acta Crystallogr. D***53**, 240–255 (1997).

40. McRee, D.E. XtalView/Xfit: a versatile program for manipulating atomic coordinates and electron density. *J. Struct. Biol.* **125**, 156–165 (1999).
41. Merritt, E.A. & Murphy, E.P. Raster3D version 2.0: a program for photorealistic molecular graphics. *Acta Crystallogr. D***50**, 869–873 (1994).

## Author contribution

T.U. purified and crystallised proteins, collected X-ray data, analysed data, and helped write the manuscript; Y.Ku. collected X-ray data; M.N. cloned the construct and helped write the paper; Y.Ki. was involved in the study design; N.T. and K.T.N. designed the study, analysed data, and helped write the paper. All the authors discussed the results, commented on the manuscript, and approved the manuscript.

## Additional information

**Supplementary Information** accompanies this paper at http://www.nature.com/scientificreports

Atomic coordinates for the reported structures have been deposited with the Protein Data Bank under accession codes 3AU8 (PfDXR-NADPH-Mn$^{2+}$), 3AU9 (PfDXR-NADPH-Mg$^{2+}$-fosmidomycin), and 3AUA (PfDXR-NADPH-Mg$^{2+}$-FR900098).

**Competing financial interests:** The authors declare no competing financial interests.

**How to cite this article:** Umeda, T. *et al.* Molecular basis of fosmidomycin's action on the human malaria parasite *Plasmodium falciparum*. *Sci. Rep.* **1**, 9; DOI:10.1038/srep00009 (2011).